Cytokine 60 (2012) 718–730

Contents lists available at SciVerse ScienceDirect

Cytokine

journal homepage: www.journals.elsevier.com/cytokine

Differential activation of the inflammasome in THP-1 cells exposed to chrysotile asbestos and Libby "six-mix" amphiboles and subsequent activation of BEAS-2B cells

Muyao Li [a], Mickey E. Gunter [b,c], Naomi K. Fukagawa [a,*]

[a] Department of Medicine, University of Vermont College of Medicine, Burlington, VT 05405, USA
[b] Department of Geological Sciences, University of Idaho, Moscow, ID 83844, USA
[c] Marsh Professor-at-Large, University of Vermont, Burlington, VT 05405, USA

ARTICLE INFO

Article history:
Received 16 February 2012
Received in revised form 28 July 2012
Accepted 27 August 2012
Available online 25 September 2012

Keywords:
Chrysotile asbestos
Libby six-mix amphiboles
Macrophage
IL-1β
Epithelium

ABSTRACT

Inflammatory responses of THP-1 cells (macrophage cell line) exposed to chrysotile asbestos (Chry) and Libby six-mix (LIB) and the subsequent impact on bronchial epithelial cells were determined. Direct treatment of THP-1 cells with Chry caused cell death, activation of caspase-1 and release of IL-1β, while the addition of caspase-1 inhibitor, Z-YVAD-FMK, reduced IL-1β, suggesting that Chry activated the caspase-1 mediated Nod-like receptor protein 3 (NLRP3) inflammasome; by comparison, LIB had less effects on all of these parameters. Expression of antioxidant enzymes, protein oxidation and nitration, and lipid peroxides in THP-1 cells treated with the two particles suggest that LIB generated more reactive oxygen species (ROS) than the same dose of Chry. Differences in fiber length and surface area suggest a possible role for particulate size in the differential activation of the inflammasome. BEAS-2B cells, representing the bronchial epithelium, treated with supernatants of medium from Chry- or LIB-treated THP-1 cells (conditioned medium) activated the MAPK cascade, increased phosphorylation of ERK and Cot (MAP3K8), increased AP-1 binding activity and induced IL-6 release. To verify that IL-1β from THP-1 cells was responsible for activation of BEAS-2B, conditioned medium with added IL-1Ra, an IL-1β antagonist, was applied to BEAS-2B. Results show that IL-1Ra attenuated effects of conditioned medium, supporting a role of IL-1β, as a secondary mediator, in the transduction of inflammatory signaling from the macrophage to epithelial cells. The effects of LIB-conditioned medium appeared to be less dependent on IL-1β. In conclusion, Chry and LIB induce differential inflammatory responses in THP-1 cells that subsequently lead to differential effects in epithelial cells.

© 2012 Elsevier Ltd. All rights reserved.

1. Introduction

Human exposure to asbestos is associated with an increased incidence of pleural disease, asbestosis, lung cancer, and mesothelioma [1]. Inflammation plays a key role in lung injury, involving different cell types, such as alveolar macrophages and bronchial epithelial cells that initiate and/or sustain inflammatory processes. Alveolar macrophages provide surveillance of the major boundaries between the body and the outside world. Macrophages are innate immune cells with well-established roles in the primary response to pathogens. These cells recognize danger signals through receptors and activate specific signaling pathways [2]. The macrophage-like cell line, THP-1, has been shown to secrete the proinflammatory cytokine, IL-1β, upon contact with crocidolite asbestos [3–5]. Mature IL-1β is processed through cleavage of the inactive pro-IL-1β precursor by caspase-1/ICE (IL-1β converting enzyme). Caspase-1 was the first caspase to be discovered in mammals, but only recently has the pathway leading to its activation been elucidated and shown to involve a series of large complexes, called inflammasomes [6,7]. Stimulation of macrophages with asbestos resulted in cell death and robust secretion of IL-1β in a manner dependent on the Nod-like receptor protein 3 (NLRP3),

Abbreviations: ASC, apoptosis-associated speck-like protein containing a CARD; Chry, chrysotile; Cot, cancer osaka thyroid oncogene; DNPH, 2,4-dinitrophenylhydrazine; EMSA, electrophoretic mobility shift assay; GB, glass beads; GCLC, γ-glutamate cysteine ligase catalytic subunit; IKKs, IκB kinases; IL-1Ra, IL-1 receptor antagonist; IL-1RAcP, IL-1 receptor accessory protein; IRAK, interleukin-1 receptor-activated protein kinase; LIB, Libby "six-mix amphiboles"; MAP3K, MAPKKK, MAPK kinase kinase; MnSOD, manganese SOD; MYD88, myeloid differentiation primary response gene 88; NLRP3, NOD-like receptor family, pryin domain containing 3; PMA, phorbol-12-myristate-13-acetate; SA, surface area; SOD, superoxide dismutase; TRAF6, TNF receptor-associated factor 6; TIR, Toll- and IL-1R-like; Tpl2, tumor progression locus 2; ZYF, Z-YVAD-FMK.

* Corresponding author. Address: Department of Medicine, University of Vermont College of Medicine, 89 Beaumont Avenue, Given C-207, Burlington, VT 05405, USA. Tel.: +1 802 656 4403; fax: +1 802 656 2636.
E-mail address: Naomi.Fukagawa@uvm.edu (N.K. Fukagawa).

1043-4666/$ - see front matter © 2012 Elsevier Ltd. All rights reserved.
http://dx.doi.org/10.1016/j.cyto.2012.08.025

also called Nalp3 (NACHT, LRR and PYD domains-containing protein 3) inflammasome [3,4,8,9]. Previous reports have indicated that macrophages from wild-type mice could undergo caspase-1-mediated IL-1β maturation but macrophages deficient in the NLRP3 inflammasome were incapable of secreting IL-1β [3,4,8].

Following the initiation of proinflammatory responses upon exposure to asbestos with the release of cytokines, such as IL-1β, alveolar macrophages often die and are cleared from the airway. In contrast, neighboring bronchial epithelial cells can sustain pathogenic responses and lead to asbestos-related lung disease, even if they may not be in direct contact with the asbestos fibers. IL-6 is considered to be an important mediator of acute inflammation [10] and implicated in the pathogenesis of particle-related lung disease. The MAPK pathways contribute to epithelial cell proliferation, which is a major risk factor for the development of lung cancer or fibro-proliferative diseases [11,12]. Whether IL-1β secreted by THP-1 cells affects the alveolar epithelium leading to cell proliferation, inflammation and eventual fibrosis via MAPK-IL-6 pathways is uncertain although it is well established that direct exposure of pulmonary epithelial cells [13], alveolar [14], and bronchial epithelial cells [15,16] to asbestos leads to activation of MAPK cascades and induction of ERK1/2 phosphorylation.

Several investigators have examined the interaction between macrophages and bronchial epithelial cells, employing a co-culture system (Transwell) in which two different cell types were separated by a membrane with only macrophages exposed to the particles of asbestos or silica [17–19]. In the other compartment, the epithelial cells were bathed by the same culture medium. Although interesting connections were suggested, the underlying mechanisms whereby primary responses of the macrophage initiated and interacted with lung epithelial cells remain unclear. We have investigated signal transduction from THP-1 macrophage-like cells to BEAS-2B bronchial epithelial cells through a relatively simple method: that is, to initially determine the inflammatory responses of THP-1 exposed to different particulate fibers followed by collection of the supernatants of culture medium without any fibers (termed as conditioned medium) in which BEAS-2B cells were then grown and their responses assessed.

Asbestos occurs naturally and is composed of long thin fibers broadly classified into two groups: serpentine and amphibole [20]. Chrysotile asbestos (the asbestiform variety of the serpentine group) is the most commonly used asbestos type in the US [21]. The amphibole asbestos group consists of five mineral species: amosite, crocidolite, tremolite, actinolite, and anthophyllite. The amphibole asbestos occurring in the vermiculite mine near Libby, Montana, is a mixture of several different species of amphiboles [22]. Several research groups have studied this material, but the samples used in the present work are a subset of those discussed in the publication by Meeker et al. [23] and morphologically characterized by Bellamy and Gunter [24]. Bellamy and Gunter referred to the Libby material as "six-mix". Because many of the studies examining the pathogenic mechanisms related to aberrant cellular responses to asbestos exposure utilized different forms of asbestos, the present work contrasts the signal transduction pathways induced by chrysotile asbestos (Chry) and Libby six-mix (LIB). The role of IL-1β in the THP-1-conditioned medium secreted in response to Chry or LIB was compared and its subsequent effects on BEAS-2B immune responses, specifically IL-6 secretion, were examined.

2. Materials and methods

2.1. Cell culture

THP-1 cells: THP-1 cells from a human monocyte cell line were grown in RPMI 1640 medium (Invitrogen) containing 10% FBS; 100 U/ml Penicillin/Streptomycin; 10 mM HEPES and 1 mM Sodium pyruvate at 37.0 °C in 5% CO_2. Cells from this monocytic cell line require differentiation into cells with the functional characteristics of mature macrophages [25,26], accomplished by treatment with 100 nM PMA overnight and then refreshing the cells with medium without PMA. *BEAS-2B cells*: BEAS-2B cells from the human bronchial epithelial cell line (ATCC) were seeded into flasks or plates pre-coated with a mixture of 0.01 mg/ml fibronectin, 0.03 mg/ml bovine collagen type I and 0.01 mg/ml bovine serum albumin in medium. The cells were grown in DMEM/F12 medium (Invitrogen) containing 10% FBS; 100 U/ml of Penicillin/Streptomycin, 1 μg/ml Insulin-Transferrin-Na selenite (Sigma), 1 μg/ml Hydrocortisone (Sigma), and 10 mM HEPES at 37.0 °C in 5% CO_2.

2.2. Chrysotile asbestos and Libby six-mix treatments

Chrysotile asbestos fibers (National Institute of Environmental Health Sciences reference sample, NIEHS), and Libby six-mix (United States Geological Service, USGS) have been physically and chemically characterized previously [21,24,27–30]. Glass beads (GB) from Polysciences Inc. were used as a noncytotoxic particle control [29]. The surface area of chrysotile measured using Micromeritics Tristar equipment for nitrogen gas sorption analysis by Happond Expander™ is reported to be 28.83 m^2/g (Table 1). The Chry and LIB fibers were sterilized under ultraviolet light overnight prior to suspension in HBSS at 1 mg/ml, sonication for 15 min in a water bath sonicator, and trituration eight times through a 22-gauge needle before treatment of the cells [31]. Two mass-based concentration systems have been commonly used in studies of asbestos exposure: (1) mass concentration, which means the mass of a constituent divided by the volume of a carrier and (2) mass-per-area, which is the mass divided by the exposed surface area. The asbestos suspensions were directly added to differentiated macrophages or BEAS-2B cells in medium at a mass concentration of 20 μg/ml and 40 μg/ml for 24 h, which was equivalent to mass per area of 5 $\mu g/cm^2$ and 10 $\mu g/cm^2$ achieved by adjusting the volume of medium based on the surface area of the culture dishes. The culture medium collected after exposure of THP-1 cells for 24 h was centrifuged at the highest speed of an Eppendorf 5430R centrifuge with 50 ml-tube rotor. Then the supernatant of medium was used to treat BEAS-2B cells and referred to as conditioned medium with indicated asbestos concentration from the original THP-1 treatment. Since the conditioned medium contained no particles and the cellular responses to GB or medium alone were similar, a GB control was not included in the experiments using conditioned medium.

2.3. Caspase-1 inhibitor treatments

A caspase-1 inhibitor VI, Z-YVAD-FMK (ZYF), was purchased from BioVison and a caspase-1 inhibitor V, Z-D-CH2-DCB (ZD), from Calbiochem. In preliminary experiments, 10, 20, 40 and 50 μM of inhibitors were applied to THP-1 cell 30 min prior to asbestos treatment. After 24 h, the inhibitory effects on production of IL-1β were compared, suggesting that ZYF was more efficient than ZD. Based on these preliminary results, only 40 μM of ZYF was used in the subsequent experiments.

2.4. IL-1β and IL-1Ra treatments

Recombinant human IL-1β protein and the antibody for cleaved IL-1β were purchased from Cell Signaling. The IL-1 receptor antagonist (IL-1Ra) was purchased from Abcam. BEAS-2B cells were challenged in preliminary experiments by 10, 20, 40, 80, and 100 ng/ml recombinant IL-1β to determine its effect on the secretion of IL-6. The inhibitory effects of both IL-1Ra and anti-IL-1β

Table 1
Fiber size references.

Fiber name	Mean fiber length (μm)	Mean SA (m^2/g)	Source
Glass beads (GB)[a]	2.06	3	Polysciences Inc
Chrysotile (Chry)	21[b]	28.83[c]	NIEHS
LIBBY-6-mix (LIB)[d]	7.21	5	USGS

[a] [29].
[b] [30].
[c] Nitrogen gas sorption analysis by Hammond Expanders™.
[d] [29].

were also tested and compared. Based on the preliminary results, only 400 ng/ml of IL-1Ra was used in the subsequent experiments to treat BEAS-2B cells.

2.5. CytoTox-Glo™ Assay viability protocol

The CytoTox-Glo™ Assay (Promega) uses a luminogenic peptide substrate (alanyl-alanylphenylalanyl-aminoluciferin; AAF-Glo™ Substrate) to measure dead-cell protease activity, which is released from cells after loss of membrane integrity. The assay is primarily designed to selectively detect dead cells; however, with the addition of the lysis reagent (provided in the kit), the CytoTox-Glo™ Assay viability protocol (by lysis) can also deliver the luminescent signal associated with the total number of cells. Cells were grown and treated as described above and then trypsinized and passed through the 40 μm mesh to break the clusters of cells and asbestos fibers. The collected cells were then loaded into a 96-well plate and the CytoTox-Glo™ Assay reagents applied to wells sequentially following the manufacturer's protocol. The luminescent signals were measured in a Synergy HT4 multi-detection microplate reader (BioTek Instruments). Viability was calculated by subtracting the luminescent signal resulting from experimental cell death from total luminescent values.

2.6. LDH cytotoxicity assay

The CytoTox 96® cytotoxicity assay is a colorimetric assay from Promega. The assay quantitatively measures lactate dehydrogenase (LDH), a stable cytosolic enzyme that is released upon cell lysis by treatments. Released LDH in culture supernatants was measured after 2, 4, 6, 8, and 24 h treatments with an enzymatic assay, which results in the conversion of a tetrazolium salt (INT) into a red formazan product. The amount of color formed is proportional to the number of lysed cells. Visible wavelength absorbance data were collected at 490 nm with the Synergy HT4 (BioTek Instruments). The results are expressed as a percentage of maximum LDH released from cells lysed by repeated freezing and thawing.

2.7. Cytokine assays

Cells were grown and treated as described above; the culture medium was then collected and centrifuged twice at 14,000 rpm in an Eppendorf 5430R centrifuge with a rotor for 1.5 ml-tubes, and the supernatants stored in −80 °C until analysis. Cytokines and chemokines were analyzed using both Bio-Plex Pro™ Assay (Bio-Rad) and Milliplex Map® Assay (Millipore). Bio-Plex-27 human cytokine kits were used in screening of cytokine responses, while Milliplex Map® custom kits were used for selected cytokines. The samples were prepared according to the manufacturer's instructions and run on the Bio-Plex suspension array system (Bio-Rad). Standard curves were calculated and samples were analyzed using the Bio-Plex Manager software version 5 (Bio-Rad).

2.8. Caspase-1 FLICA assay

Z-YVAD-FMK caspase-1 FLICA kit was purchased from Immunochemistry Technologies, LLC. The methodology is based on a fluorochrome inhibitor of caspase-1, the FLICA reagent FAM-YVAD-FMK, which enters the cells and binds covalently only to the active caspase-1. The asbestos-treated THP-1 cells were trypsinized and passed through the 40 μm mesh. 300 μl of each cell suspension, which contained at least 1×10^6 cells, were transferred to sterile tubes and incubated or washed sequentially with FLICA reagents according to the manufacturer's protocol. The aliquots of cells were then loaded into microtiter plate wells in different dilutions and fluorescence read on a Synergy HT4 with excitation range from 488 to 492 nm, and emission range from 515 to 535 nm.

2.9. Western-blot analysis

The antibodies for total or phospho-ERK1/2, caspase-1, total or phospho-NF-κB p65 (S536) were purchased from Cell Signaling; the antibody for total Cot from Santa Cruz; the antibodies for phospho-Cot (T290), β-actin and α-tubulin from Abcam Inc.; the antibodies for MnSOD, GCLC from Abnova; the antibody for NLRP3 from AdipoGen; the antibody for 3-nitrotyrosine from Millipore. Total or nuclear proteins were extracted from treated cells as described previously [32]. The 20 μg of each total protein was electrophoresed on 10% or 7.5% Mini-PROTEAN® TGX™ precast gels (Bio-Rad) and then electroblotted onto nitrocellulose membranes. After blocking the membranes with 1% BSA blocking/dilution buffer, the membranes were incubated with the appropriate primary antibody at the recommended concentration overnight with shaking at 4 °C and then rinsed. After incubation with corresponding secondary antibodies, the protein bands were visualized using a SuperSignal™ West Pico Trial Kit (PIERCE) and exposed to radiographic films. The images and densities were captured with a GS-700 Imaging Densitometer (Bio-Rad, Richmond, CA) and analyzed with Quantity One Software Version 4.2 (Bio-Rad, Richmond, CA). The membranes were stripped and then reimmunoblotted with another antibody or loading control: β-actin or α-tubulin antibody.

2.10. Oxidized protein detection

Protein carbonyl modifications were detected and quantified using the OxyBLOT™ Assay (Millipore) according the manufacturer's protocol. Briefly, BEAS-2B cells were treated with Chry and LIB and protein lysates were incubated with 2, 4-dinitrophenylhydrazine (DNPH). The DNP-derivative protein samples were separated by SDS–PAGE followed by Western blotting. The same membranes were stripped and then reimmunoblotted with β-actin as a loading control.

2.11. Lipid and aqueous peroxides assay

Lipid and aqueous peroxides in THP-1 conditioned medium were measured with the OxiSelect™ Hydrogen Peroxide Assay Kit (Cell Biolabs, Inc.) according to the manufacturer's protocol. Peroxide in the medium converts Fe^{2+} into Fe^{3+}, which reacts with an equal molar amount in the presence of acid to create a purple product that absorbs maximally between 540 and 600 nm. Samples were then reacted with xylenol orange in 96-well plate and read on the Synergy HT4. The peroxide content in unknown samples was calculated by comparison with the predetermined H_2O_2 standard curve.

2.12. EMSA for AP-1

Double stranded AP-1 consensus oligonucleotides were purchased from Promega. The probes were labeled with [γ-^{32}P] ATP using T4 polynucleotide kinase (Invitrogen) according to the manufacturer's protocol. EMSA was performed as described previously [33]. The 6 μg of nuclear extracts from BEAS-2B cells exposed to Chry, LIB or 10 ng/ml of TNF-α were used in the binding assay; 1 μl of anti c-Fos antibody (Santa Cruz) were applied to supershift the AP-1 complexes, respectively; cold AP-1 probes were also included at 1:100 M ratios for probe competition.

2.13. Statistics

Values are presented as mean ± SEM for indicated numbers of experiments, or mean ± SD for measurement with replicates. The mean values are reported as a percentage of control. Comparisons were performed using one way Anova (GraphPad). The p values were considered to be significant if they were $\leqslant 0.05$.

3. Results

3.1. Cell viability in response to asbestos exposure

Cell viabilities were assessed with the CytoTox-Glo™ Assay and results shown in Fig. 1A and B. Differences between the two cell lines were found in the responses to direct exposure of THP-1 and BEAS-2B cells to 20 or 40 μg/ml of Chry (Chry20, Chry40) and LIB (Lib20, Lib40). After 24 h of exposure, Chry significantly reduced the survival of THP-I cells compared to control, whereas LIB had less of an effect (Fig. 1A). No reduction of cell viability was seen in BEAS-2B cells with the treatments compared to control; however, cell number based on the CytoTox-Glo™ Assay slightly increased with LIB treatments (Fig. 1B). To confirm the result from Fig. 1A, a LDH cytotoxicity assay was used in THP cells treated with Chry and LIB for 2, 4, 6, 8, and 24 h (Fig. 1C). Cell death gradually increased with increasing exposure times. By 24 h, Chry40 had induced significant cell death (~60%), with lesser degrees induced by Chry20, LIB40 and LIB20. Together the data indicate selective cytotoxicity in macrophages exposed to asbestos compared to epithelial cells.

3.2. IL-1β and caspase-1 responses in THP-1 cells

Cytokine and chemokine concentrations were measured in the supernatant of the culture medium from treated THP-1 cells using the human Bio-Plex array (see Supplementary Tables 1 and 2 for complete set of data). IL-1β was the most prominently induced cytokine. Fig. 2A shows the results of induction of IL-1β in 3 independent experiments when THP-1 cells were treated with Chry and LIB for 24 h. Chry20 induced a 4-fold and Chry40 a 6-fold increase in IL-1β secretion compared to the control; whereas Lib40 induced IL-1β secretion by only 2.9-fold. Meanwhile GB and control resulted in similar levels of IL-1β. Other cytokines found to be significantly induced included IL-1Ra, G-CSF and IL-2 (see Supplementary Table 2).

The combination of cell death and IL-1β secretion suggested the possible involvement of NLRP3 inflammasome activation. NLRP3 expression was hence determined by Western-blot and showed that NLRP3 protein level was higher in all treatments compared to control. However, none of treatments achieved statistical significance compared to control (Fig. 2B).

Pro-caspase-1, an assembling member of the inflammasome complex, is proteolytically activated from a proenzyme to produce two active subunits, p20 and p10, with p20 being identifiable by immuno-blotting. Fig. 3A shows a representative blot and a summary of data obtained from three independent experiments. Results suggest that active p20 was induced by the Chry treatments, especially Chry40, but to a lesser degree by LIB treatments with no effect by GB. To further confirm the activation of caspase-1 in Chry-treatments, the caspase-1 FLICA assay was performed and the result revealed that Chry40 clearly increased caspase-1 activity in the THP-1 cells (Fig. 3B).

The activation of caspase-1 and secretion of IL-1β are two important consequences of inflammasome activation. To verify whether blocking caspase-1 activation would reduce maturation of IL-1β in macrophages, a caspase-1 inhibitor, Z-YVAD-FMK (ZYF) was used in PMA-differentiated THP-1 cells and treated with 40 μg/ml asbestos. Application of ZYF showed a trend towards

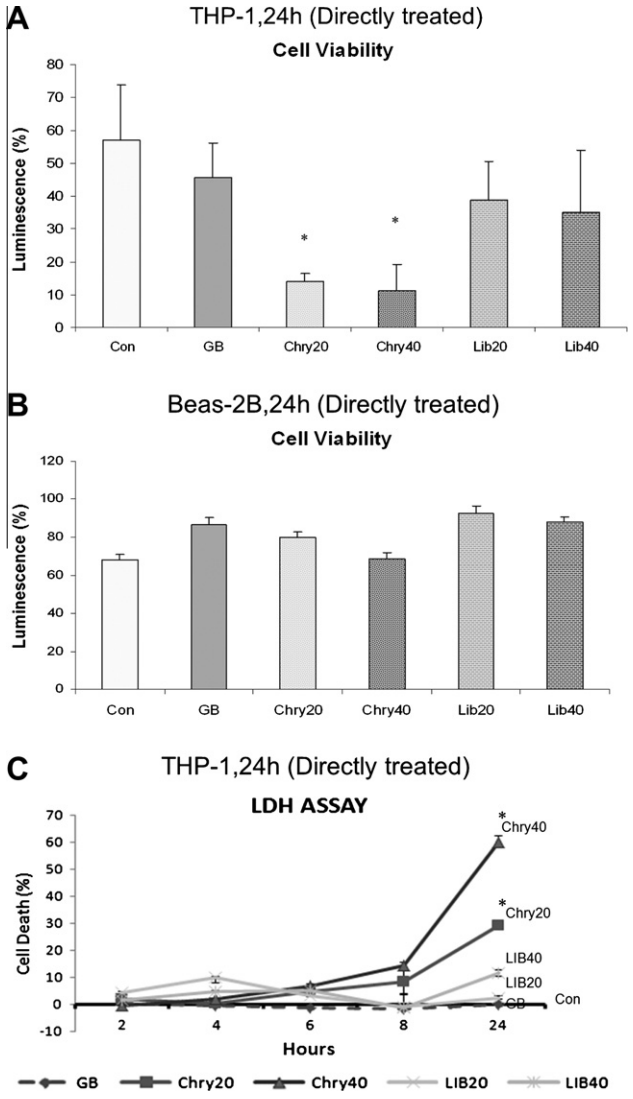

Fig. 1. Cell viability and cytotoxicity. THP-1 cells differentiated with 100 nM PMA were refreshed and exposed to 20 μg/ml or 40 μg/ml of chrysotile (Chry20, Chry40) and LIB (Lib20, Lib40), and 40 μg/ml glass beads (GB). (A) Cell viability was measured using the CytoTox-Glo™ viability protocol in duplicate after 24 h treatments. The results were calculated by subtracting the luminescent signal resulting from experimental cell death based on total luminescent values. (B) BEAS-2B cells were treated with Chry20, Chry40, Lib20, Lib40 and GB. Cell viability was measured after 24 h treatments using the CytoTox-Glo™ viability protocol in duplicate. (C) Cytotoxicity in the THP-1 cells was determined with the LDH cytotoxicity assay in duplicate and over a 2, 4, 6, 8 and 24 h time course. Results were expressed as a percentage of maximum LDH released from cells lysed by repeated freezing and thawing. * Indicates $p \leqslant 0.05$ when comparing treatments to control.

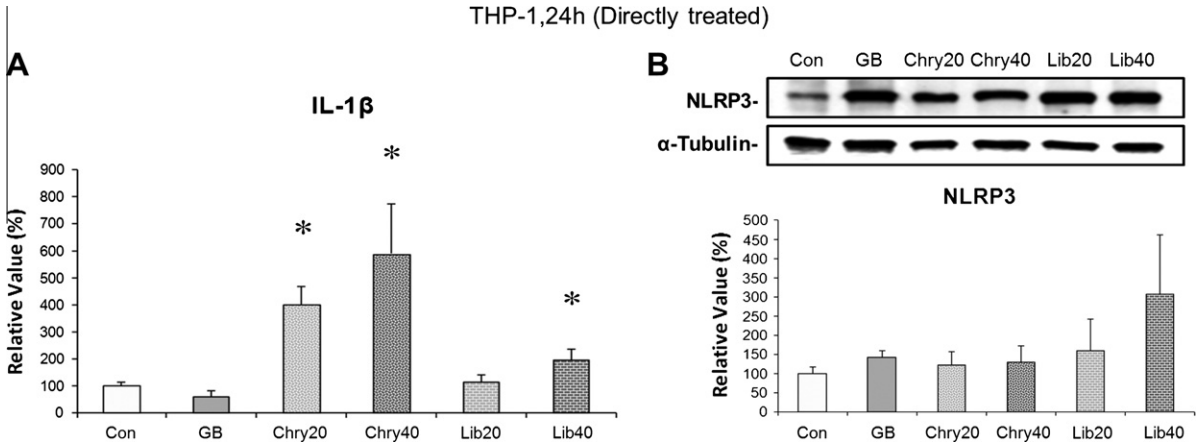

Fig. 2. IL_1β release and NLRP3 priming. (A) Release of IL-1β in THP-1 cells was analyzed with a Bio-Plex 27 cytokine array. THP-1 cells were grown and treated with Chry and LIB for 24 h as described; the supernatant of culture medium was collected and then analyzed. Results from three independent experiments were summarized as mean ± SE in the bar-graphs. * Indicates $p \leqslant 0.05$ when comparing asbestos treatments with control. (B) NLRP3 expression in Chry and LIB treated THP-1 cells. A representative Western-blot in the upper panel showing induction of NLRP3 levels with α-tubulin as a loading control. The lower panel is a summary bar-graph from three independent blots.

repression of active p20, although the inhibitory effect did not reach statistical significance (Fig. 3A). Meanwhile, Fig. 3C shows that IL-1β was significantly induced by Chry20 and Chry40 with less effect of Lib40 and no effect of GB. ZYF significantly repressed the Chry40 and Lib40 effects resulting in little IL-1β detectable in the medium. These results suggest that IL-1β secretion in response to asbestos is caspase-1 dependent.

3.3. Comparison of ROS production in Chry and LIB treated THP-1 cells

Oxidative stress is another potential mediator for particle-induced inflammation in cells. Two antioxidant related enzymes, superoxide dismutase (SOD) and γ-glutamate cysteine ligase catalytic subunit (GCLC), were selected as the indicators of oxidative status since SOD expression is often low in the presence of oxidative stress whereas GCLC expression is induced if cells are challenged by a reduction in GSH levels. Blake et al. have reported in murine macrophages that internalization of LIB asbestos fibers generated a significant increase in intracellular ROS, decreased GSH levels, and impaired total SOD activity [34]. To clarify the oxidative stress status in Chry- and LIB- treated THP-1 cells, the expression of manganese SOD (MnSOD) and GCLC were compared by Western blots. The upper panel of Fig. 4A shows protein blots of the two enzymes in THP-1 cells treated with either Chry or LIB; the

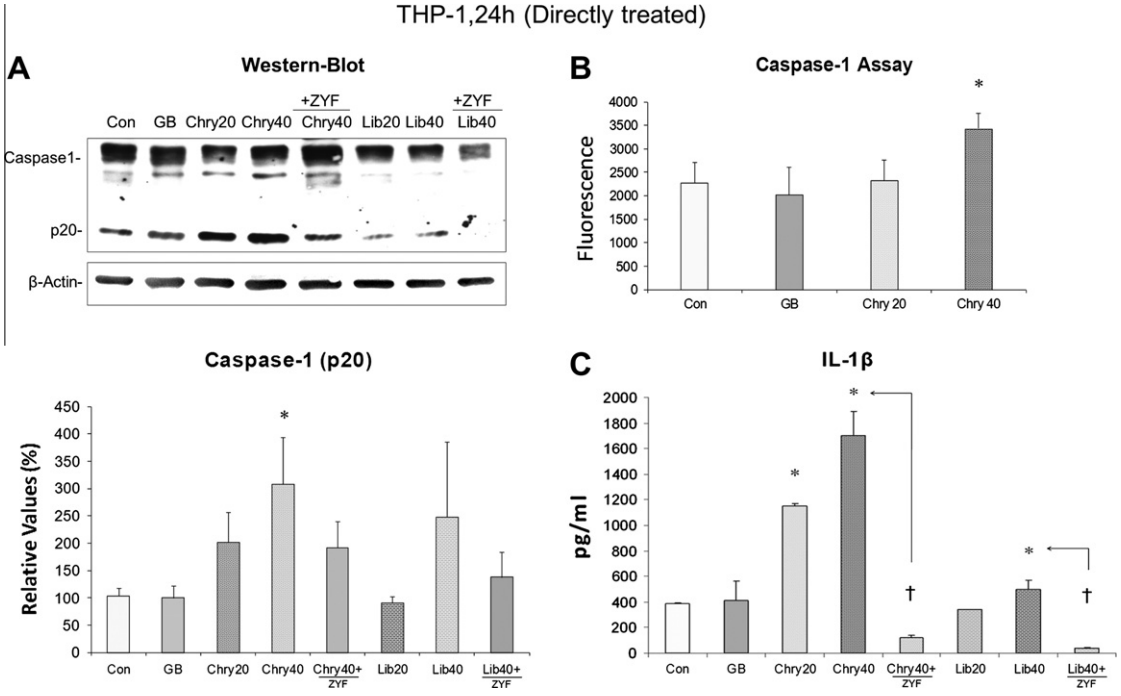

Fig. 3. Activation of caspase-1. (A) Representative Western blot in the upper panel showing both active p20 subunits and other caspase-1 protein components in Chry- and LIB- treated THP-1 cells; Chry40 and Lib40 were applied with or without caspase-1 inhibitor, ZYF. β-actin in the same blot served as a loading control. The lower panel in (A) is a bar-graph summarizing three independent blots (mean ± SE) and * indicates $p \leqslant 0.05$ when comparing Chry treatments with control. (B) Measurement of caspase-1 activity with the Z-YVAD-FMK caspase-1 FLICA kit. Chry treated THP-1 macrophages were analyzed for casepase-1 activity in triplicate (values are mean ± SD), * indicates $p \leqslant 0.05$ when comparing Chry treatments with control. (C) The effects of ZYF on release of IL-1β by the THP-1 cells. The 40 μM of caspase-1 inhibitor, ZYF, was applied to THP-1 cells 30 min prior to exposure to Chry and LIB. IL-1β levels in media analyzed with Milliplex Plex-2 Assay in triplicate (values are mean ± SD), * indicates $p \leqslant 0.05$ when comparing Chry or LIB treatments with control; † indicates $p \leqslant 0.05$ when comparing ZYF-treated vs. non-ZYF treated cells exposed to Chry and Lib.

lower bar-graphs summarizes MnSOD and GCLC expression in three experiments. Induction of MnSOD was found in response to Chry but not seen in GB and LIB-treated cells. Meanwhile, an increase of GCLC was seen in LIB treated cells but there was little in GB and Chry-treated cells. The difference between the responses to Chry and LIB treatments suggests that the two particulates induced oxidative stress to different degrees. Protein carbonyl modifications were then determined using the OxyBLOT™ Assay. A representative blot (Fig. 4B) shows that THP-1 cells treated with Lib40 displayed a dramatic increase in the number and degree of oxidized proteins as compared to control, GB and Chry40-treated cells. This suggests that more oxidative stress is generated by LIB amphiboles compared to Chry. Reactive nitrogen species is another indicator of oxidative stress. Protein tyrosine nitration in Chry- and LIB- treated THP-1 cells was also compared and shown in a representative blot in Fig. 4C. LIB induced more 3-nitrotyrosine formation than Chry treatments. Finally, the existence of lipid peroxides in conditioned medium was evaluated with the OxiSelect™ Hydrogen Peroxide Assay as shown in Fig. 4D. LIB treatments resulted in more lipid peroxide in conditioned medium than Chry treatments with most of the peroxide found in the lipid rather than aqueous fraction. There was a significant difference between the responses to Lib20 compared to Chry20.

3.4. Role of IL-1β in BEAS-2B responses to THP-1-conditioned medium

BEAS-2B cells were directly treated with Chry and LIB for 24 h. The induction of IL-6 by direct exposure of epithelial cells to Chry has been described elsewhere [17,35]; therefore in the present work, Chry-40 was used as a "positive control". IL-6 was found to be significantly induced by Chry40 and less so by Lib40 in directly treated BEAS-2B cells, as shown in Fig. 5A.

BEAS-2B cells were then grown in THP-1 conditioned medium for 24 h as well. Because the IL-1β levels in GB-conditioned medium was consistent with control, as described in Section 3.2, GB-conditioned medium was not used in the conditionally treated BEAS-2B cells. Several cytokines were found to be induced by conditioned medium (see Supplementary Tables 1 and 2). The most significant change occurred in IL-6 levels as shown in Fig. 5B. In comparison to Fig. 5A, direct treatment with Chry40 induced a 4.8-fold increase of IL-6 compared to control; whereas the increase in IL-6 by Chry40-conditioned medium was only 1.5-fold. The increase in IL-6 by LIB-conditioned medium was less than seen with Chry-conditioned medium. These data support the contention that induction of IL-6 by THP-1 conditioned medium may be related to IL-1β.

Activation of the MAPK cascade is a prominent finding in epithelial cells directly treated with asbestos [16,36]. Recently, another inflammatory protein kinase, Cot (cancer osaka thyroid oncogene), which is also known as Tpl2 (tumor progression locus 2) or MAP3K8 and functions upstream of MAPK signaling has been described [37]. BEAS-2B cells directly treated with Chry and LIB particles showed increased phosphorylation of ERK1/2 and phosphorylation of Cot kinase at Tyr290 compared to control (see Supplementary Fig. 1A and B). To determine whether conditioned medium had the same stimulatory function as directly treated BEAS-2B cells, activation of ERK and Cot was examined in BEAS-2B cells treated with THP-1 conditioned medium. Fig. 6A shows induction of P-ERK and P-Cot by Chry- and LIB-conditioned medium, similar to effects seen in directly treated cells.

Since the transcription factor NF-κB has also been suggested to play a key role in the regulation of IL-6 expression and IL-1β is known to specifically induce phosphorylation of NF-κB p65 at Ser536 [38], the phosphorylation status of NF-κB p65 at Ser536 was also examined in conditionally treated BEAS-2B cells. The results revealed that phosphorylation of NF-κB p65 at Ser536 was induced by Chry40-conditioned medium (Fig. 6B). Activation of AP-1, which is downstream of MAPK pathways, is another important feature of asbestos-treated epithelial cells. Thus, the binding activity of AP-1 was compared by EMSA, as shown in Fig. 6C, and demonstrated that the binding activity of AP-1 was augmented by both Chry40 and Lib20 conditioned medium.

To determine if IL-1β itself could activate BEAS-2B cells to secrete IL-6 as it appears to have done with conditioned medium, we treated cells with recombinant human IL-1β protein. IL-1Ra, an antagonist protein of IL-1β, was also used in parallel to test its effect on inhibition of IL-1β. Fig. 7A summarizes the IL-1β effect on IL-6 secretion. Treatment of BEAS-2B with 10 ng/ml of IL-1β induced ~1.6-fold increase in IL-6 secretion compared to control, but increasing the dose beyond 10 ng/ml did not show a dose-dependent increase of IL-6 (data not shown). The effect of 100 ng/ml of IL-1β on IL-6 was even lower than the effect of 10 ng/ml. This finding is consistent with an effective dose in pharmacology (ED50) where the ED50 of recombinant IL-1β is commonly reported to be much less than 10 ng/ml. The IL-1Ra molecule is structurally related to IL-1β but has mutations rendering it incapable of forming a complex with IL-1β/IL-1RI/IL-1 receptor accessory protein (IL-1RAcP) [39]. IL-1Ra-treatment did successfully suppress IL-6 secretion.

Although BEAS-2B cells treated with conditioned medium did not have direct contact with asbestos fibers, both direct and conditioned medium treatments resulted in phosphorylation of MAPK and secretion of IL-6. In addition, IL-1β itself can stimulate BEAS-2B in the same manner. The component in the conditioned medium that mediated the inflammatory message from THP-1 cells to BEAS-2B cells is likely to be IL-1β. The specificity of the IL-1β effect in conditioned medium was hence tested by IL-1Ra to see whether IL-1Ra competitively blocked IL-1β in the conditioned medium and consequently affected the cellular responses of BEAS-2B cells. BEAS-2B cells were treated with THP-1-conditioned medium, in addition to Chry40 and Lib40 with or without 40 μM of ZYF (Chry40, Chry40 + ZYF, Lib40, Lib40 + ZYF) for 24 h. 400 ng/ml of IL-1Ra inhibitor was added to another set of Chry40- or Lib40-conditioned media (Chry40 + IL-1Ra, Lib40 + IL-1Ra). Fig. 7B illustrates the corresponding changes in IL-6 by the Milli-Plex 2 Assay done in triplicate. Conditioned medium of Chry40 + ZYF slightly decreased IL-6; however, addition of IL-1Ra to Chry40-conditioned medium had a much greater effect on the suppression of IL-6 release. In contrast, LIB treatments showed the same trends, but none of the differences reached significance. Fig. 7C shows a representative of Western-blots on the top and two summary graphs below. Results in Fig. 7C indicates the same trend of the inhibitory effects of IL-1Ra on the phosphorylation of ERK1/2 and Cot by Chry40-conditioned medium.

In summary, both IL-6 and MAPK results demonstrate that blocking of IL-1β leads to down-regulation of the effects of Chry40-conditioned medium on BEAS-2B. This suggests that IL-1β in Chry-conditioned medium is responsible for triggering inflammatory responses in BEAS-2B cells. In contrast, blocking of IL-1β appears to play a smaller role in the effects induced by LIB.

3.5. Comparison of cytotoxicity and inflammatory effects based on matched surface area

We have compared the effects of Chry and LIB using mass concentrations of 20 and 40 μg/ml that is equivalent to mass-per-area of 5 and 10 $\mu g/cm^2$. To further evaluate whether the total surface area (SA) of particles affected the respective responses, the other approach which measures "the total surface area per unit of cross-sectional area" was also examined. According to the referenced SA values shown in Table 1, the SA of Chry is 28.83 m^2/g, Lib-by-6 mix is 5 m^2/g, and the GB control is 3 m^2/g. Two

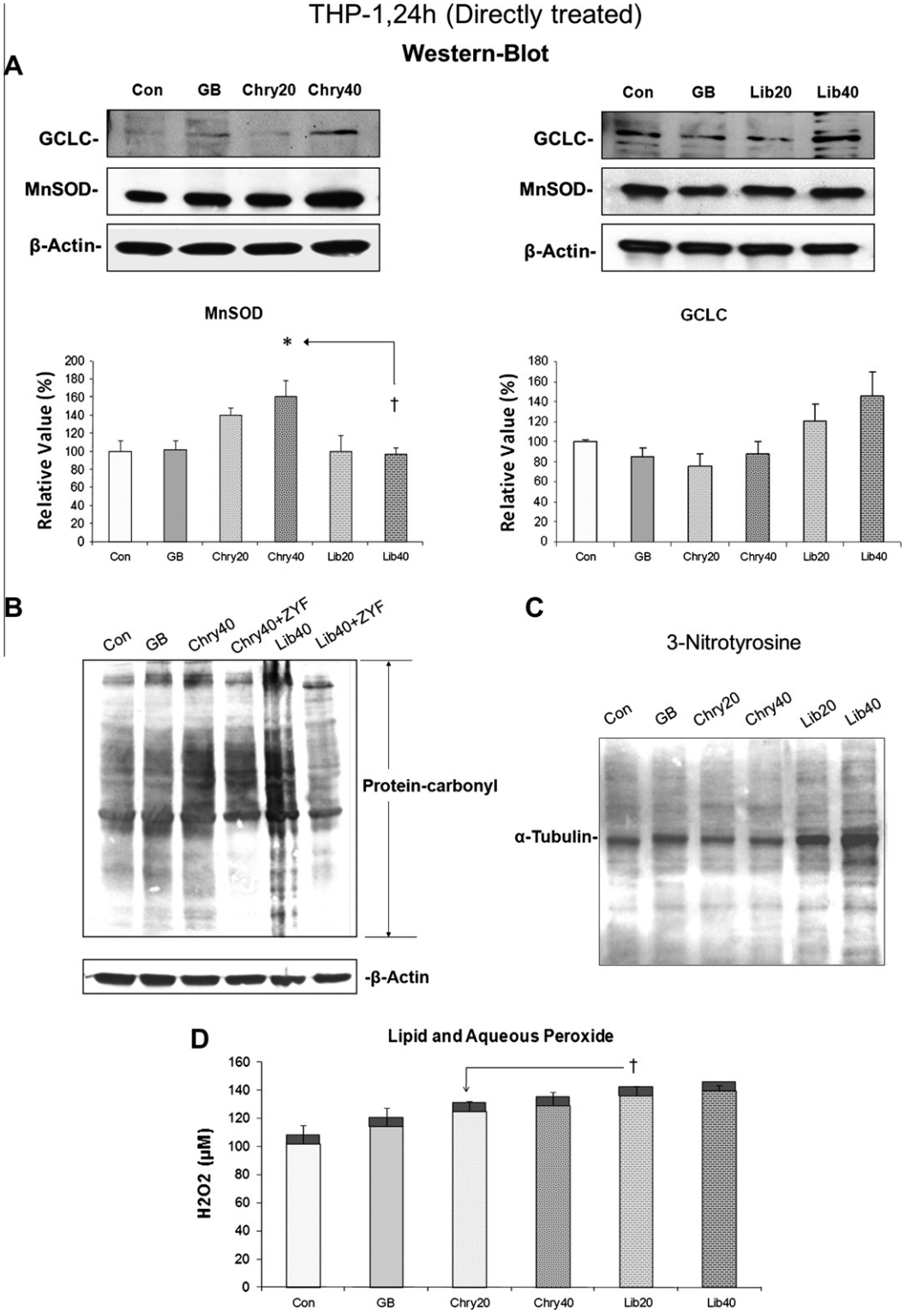

Fig. 4. Redox status in Chry and LIB treated THP-1 cells. THP-1 cells were treated with Chry and LIB for 24 h. (A) Protein levels of two antioxidant-related enzymes, MnSOD and GCLC, were evaluated by Western blots. The upper panel shows two representative blots for Chry and LIB separately with β-actin as a loading control; the lower panel shows two bar-graphs illustrating MnSOD and GCLC expression, respectively. Data are from 3 independent experiments (mean ± SE). * Indicates $p \leqslant 0.05$ when comparing Chry or LIB treatments with control; † indicates $p \leqslant 0.05$ when comparing LIB with the same dose of Chry. (B) Protein carbonyl modification after 40 μg/ml of Chry and LIB treatments with or without ZYF detected by the OxyBLOT™ Assay. A representative blot showing multiple dark bands of oxidized proteins. β-actin in the same blot serves as a loading control. (C) Nitrated proteins were detected by anti 3-nitrotyrosine antibody. A representative Western blot shows multiple dark bands for tyrosine nitration. The membrane was re-blotted with α-tubulin as a loading control. (D) Lipid and aqueous peroxide in THP-1 conditional medium analyzed by the OxiSelect Hydrogen Peroxide assay in triplicate (values are mean ± SD); the upper dark box shows the aqueous part, the lower textured box shows the lipid fraction. * Indicates $p \leqslant 0.05$ when comparing Chry or LIB treatments with control; † indicates $p \leqslant 0.05$ when comparing LIB with the same dose of Chry.

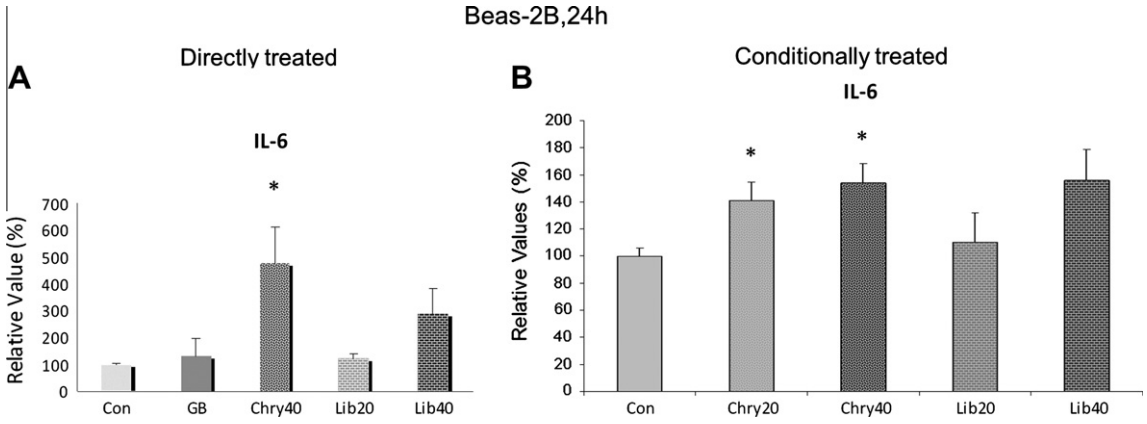

Fig. 5. Secretion of IL-6 in both directly and conditionally treated BEAS-2B cells. BEAS-2B cells were either directly or conditionally treated with Chry and LIB as described in the methods. Secretion of IL-6 was analyzed by the Bio-Plex-27 human cytokine kit. (A) IL-6 levels relative to control in directly treated BEAS-2B cells; (B) IL-6 levels relative to control in conditionally treated BEAS-2B. Each bar-graph summarizes three independent experiments (mean ± SE) and * indicates $p \leqslant 0.05$ compared to control.

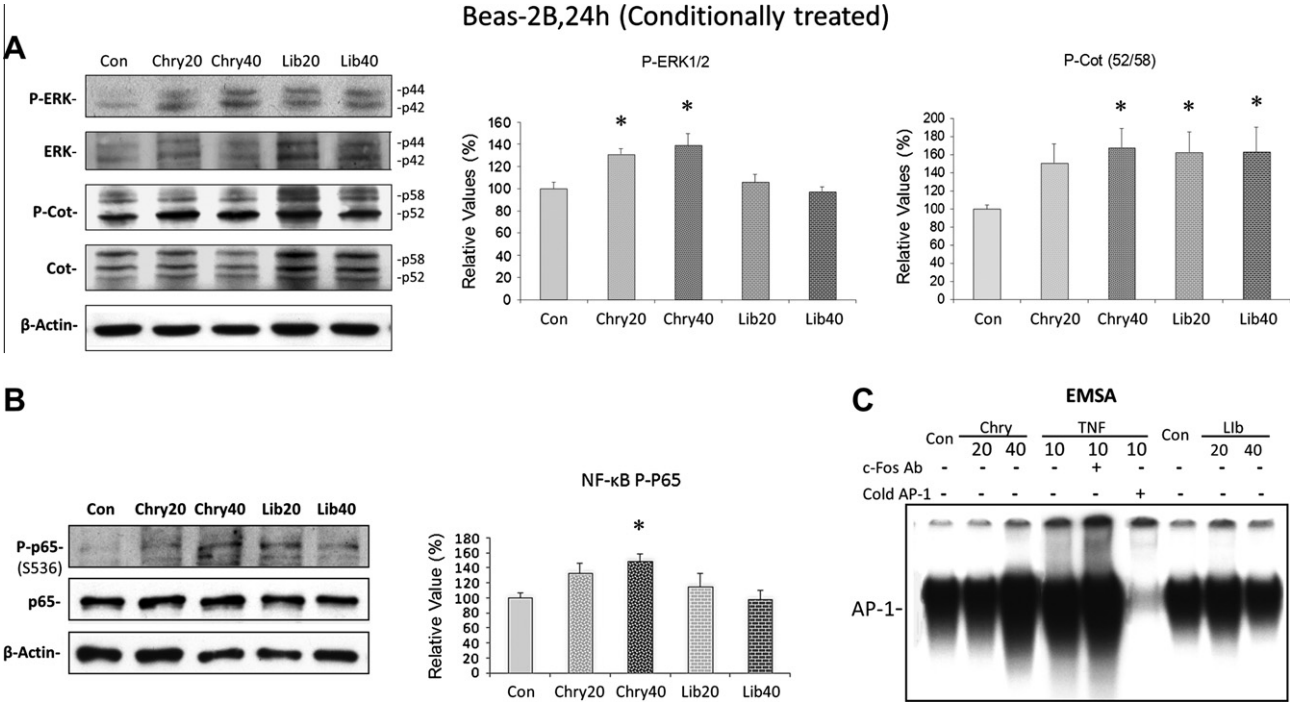

Fig. 6. Activation of ERK, Cot, NF-κB, and AP-1 in BEAS-2B cells. BEAS-2B cells were conditionally treated as described in the methods. (A) The phosphorylation of ERK1/2 (Thr202/Tyr204) and Cot (Tyr290) was detected by Western blots. Representative blots show either phosphorylated or total ERK and Cot on the left, with β-actin as a loading control; two bar-graphs summarizing 3 independent experiments (mean ± SE) are shown on the right, * indicates $p \leqslant 0.05$ compared with the control. (B) The phosphorylation of NF-κB p65 at Ser536 was detected by Western blots. Representative blot showing either phosphorylated or total and re-probed with β-actin. The bar-graph summarizing 3 independent experiments (mean ± SE) is shown on the right, (C) representative EMSA from conditionally treated BEAS-2B cells displaying AP-1 binding activities. 10 ng/ml of TNF treatment was used as a positive control.

concentrations of the total SA per area were selected that allow us to compare them to the other concentrations used. One is 25×10^6 μm^2/cm^2, which is equivalent to a mass concentration of 3.3 μg/ml Chry or 20 μg/ml LIB; the other is 150×10^6 μm^2/cm^2, which is equivalent to mass concentration of 20 μg/ml Chry or 120 μg/ml LIB. Cell viability and cytokine/chemokine secretion were again compared. Fig. 8A and B illustrates cell viability resulting from the same total surface area of Chry and LIB fibers in per cm^2 of exposed THP-1 or BEAS-2B cells. Fig. 8A shows that both fibers have a dose-dependent cytotoxic effect on THP-1 cells but that the effect of Chry150 was much greater than Lib150. Meanwhile, Fig. 8B shows that both Chry and LIB induced similar trends in responses of BEAS-2B cells where both resulted in minimal cytotoxicity of these cells. Fig. 8C and D compared the release of IL-1β by THP-1 cells and IL-6 by BEAS-2B cells respectively. Although both particles had shown similar trends of cytotoxicity, Chry elicited a totally different inflammatory response than LIB. Release of IL-1β in Fig. 8C was dramatically increased in Chry150 with an opposite effect with Lib150, suggesting that Chry150 resulted in an inflammatory form of cell death with increased cytokines; whereas Lib150 resulted in a cell death without inflammation. Similarly, Fig. 8D shows that secretion of IL-6 for the Chry150 was also quite

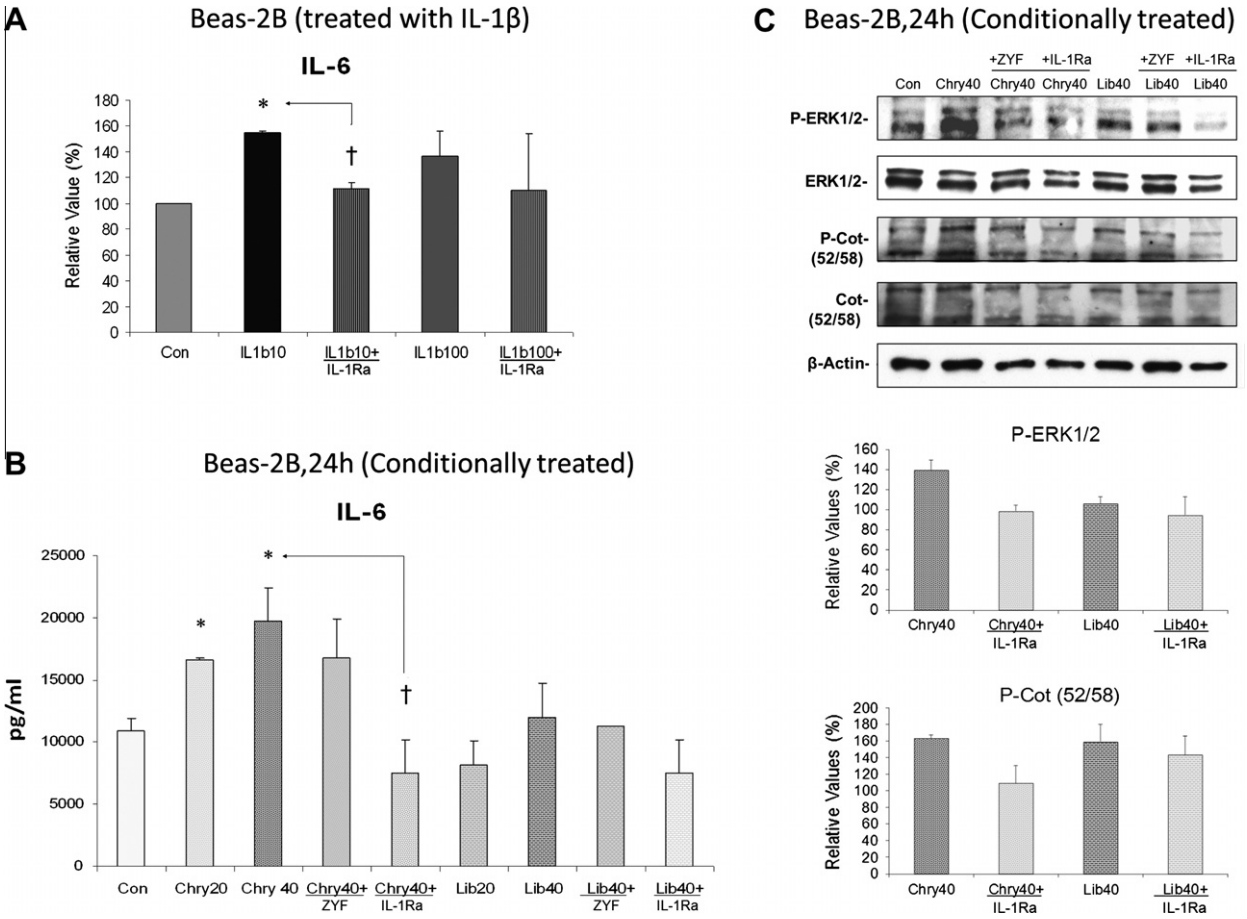

Fig. 7. Blocking the effects of IL-1β by IL-1Ra in BEAS-2B cells. (A) BEAS-2B cells were treated with 10 or 100 ng/ml of recombinant human IL-1β protein with or without 400 ng/ml of IL-1Ra, bar-graph summarizes the effects of IL-1β and IL-1Ra on BEAS-2B release of IL-6 from three individual cytokine assays (mean ± SE). (B) BEAS-2B cells were treated with conditioned medium for 24 h; the inhibitory effect of IL-1Ra on IL-6 secretion was measured by a Milli-Plex 2 assay in triplicate (mean ± SD). "Chry40 + IL-1Ra" or "Lib40 + IL-1Ra" means that 400 ng/ml of IL-1Ra was added to Chry40 or Lib40 conditioned medium before using for the treatment of BEAS-2B cells * Indicates $p \leqslant 0.05$ for Chry or LIB conditioned treatment compared to control. † indicates $p \leqslant 0.05$ for comparison between Chry40 and Lib40 conditioned treatments with or without IL-1Ra. (C) Top panel is a representative Western blot showing the inhibitory effects of IL-1Ra on phosphorylation of ERK1/2 and Cot. with β-actin as a loading control. Lower panel shows two graphs (mean ± SE) summarizing the phosphorylation of ERK1/2 and Cot in both Chry40 and Lib40 conditionally treated cells respectively, with or without IL-1Ra inhibitor.

different from Lib150. These data suggest that Chry had a much greater effect on IL-1β and IL-6 secretion than LIB, which was independent of matched total surface area.

4. Discussion

4.1. IL-1β acts as a secondary mediator

The present data elucidate the role of IL-1β in the primary responses of the macrophage and its interaction with epithelial cells as follows: (1) when exposed to Chry and LIB, THP-1 cells underwent a caspase-1 mediated inflammasome activation that resulted in an inflammatory form of cell death which now known as pyroptosis [40] and produced the proinflammatory cytokine, IL-1β; (2) exogenous IL-1β treatment activated BEAS-2B and triggered BEAS-2B inflammatory responses; (3) THP-1 conditioned medium, containing secreted IL-1β, mimicked the effect of IL-1β treatment; and (4) blocking IL-1β by IL-1Ra antagonist protein diminished the effects of conditioned medium on BEAS-2B. Together, it appears that the IL-1β in THP-1 conditioned medium acts as the secondary mediator that stimulates the BEAS-2B immune response to Chry and LIB.

However, activation of target cells by IL-1β is tightly regulated at many levels, both extracellularly and intracellularly [39,41]. The extracellular regulation includes the presence of naturally occurring inhibitors, such as the receptor antagonist, IL-1Ra. In addition to the release of IL-1β, THP-1 cells also released IL-1Ra simultaneously, as shown in Supplementary Tables 1 and 2. Thus, the effect of endogenous IL-1β in THP-1 conditioned medium was naturally restricted when it was applied to BEAS-2B cells. All of these inhibitory effects could explain why a dramatic 10-fold higher level of IL-1β in THP-1 conditioned medium treated with Chry40 was limited to only 1.5-fold greater release of IL-6 by BEAS-2B cells.

4.2. Chry and LIB differentially activate the inflammasome in THP-1 cells

In the present work, through comparison of THP-1 cells responses to Chry with LIB, we demonstrated that chrysotile asbestos has more effect on the activation of the NLRP3 inflammasome than LIB. Although Fig. 2B did not show that the NLRP3 expression in Chry treatments is higher than in LIB, activation of caspase-1 and release of IL-1β were greater in Chry than LIB treatments. NLRP3 inflammasome activation has been defined as a rapid process in which caspase-1 cleavage is induced. The process is independent of upstream de novo transcription [42]. Cell priming through multiple signaling receptors that induce NLRP3 expression is necessary

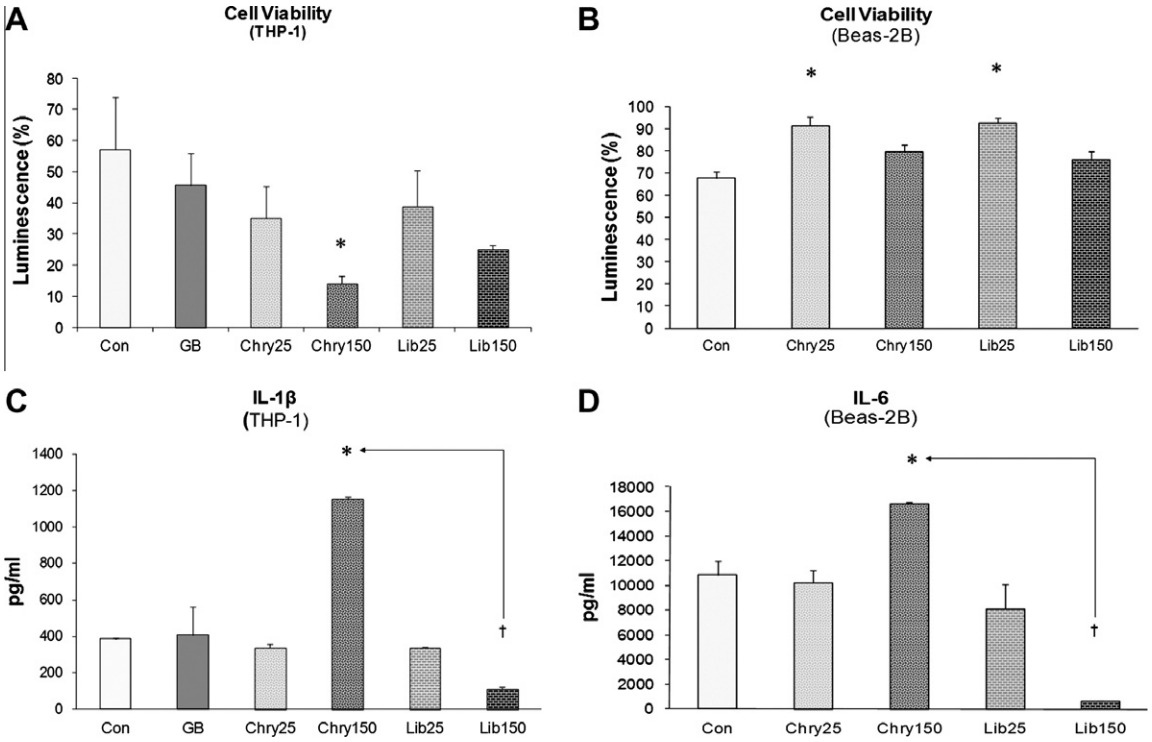

Fig. 8. Comparison of cell viability and pro-inflammatory cytokines with two matched SA/area concentrations (25 and 150 $\mu m^2/cm^2$). Cell viability assay and cytokine assay were run in duplicate, * indicates $p \leqslant 0.05$ for comparison between Chry or LIB exposure and the control. † indicates $p \leqslant 0.05$ when comparison between Chry and the same dose of LIB. (A) Cell viability in THP-1 cells. (B) Cell viability in BEAS-2B cells. (C) Secretion of IL-1β by THP-1 cells. (D) Secretion of IL-6 by BEAS-2B cells.

but not sufficient for NLRP3 activation [43]. This priming can be overcome solely by constitutive NLRP3 expression. Actually, macrophages appear to express high levels of NLRP3 constitutively and can bypass the requirement of NLRP3 expression [44,45]. Therefore, it is the activation of caspase-1, rather than expression of NLRP3, that is a key indicator of activation of NLRP3 inflammasome in THP-1 cells.

Environmental toxicants (such as asbestos) and damage-associated molecular patterns (DAMPs) activate the NLRP3 inflammasome, but the mechanisms by which these structurally distinct molecules trigger NLRP3 oligomerization and inflammasome activation are currently unclear and have been intensely debated in the literature [46]. A model in which the generation of ROS is one of the crucial elements for NLRP3 activation has been suggested [47]. However, recent studies in mice and humans defective in the generation of ROS failed to support this hypothesis and strongly suggested anti-inflammatory effects of ROS [48,49]. Furthermore, SOD was reported to be required for the activation of caspase-1; SOD1 deficiency led to more ROS in macrophages but caused caspase-1 inhibition by specific oxidation and glutathionylation [50].

In this study, Chry did not generate more intracellular ROS than LIB (Fig. 4), which was associated with more protein oxidation and tyrosine nitration. In addition, Chry promoted production of MnSOD protein but LIB did not. It seems unlikely that ROS were driving activation of the inflammasome in Chry treated THP-1 cells.

However, an alternative model of inflammasome activation that takes into account the size of the activators is the lysosome rupture model, which is particularly useful in explaining NLRP3 inflammasome activation by large particulate activators, such as Chry. According to this model, when phagocytosed particulates are too large to be efficiently cleared, inefficient clearance of the activating particle following phagocytosis leads to phagosomal destabilization and lysosomal rupture [47]. Lysosomal damage results in the release of lysosomal proteases into the cytosol that mediates NLRP3 inflammasome activation [51,52]. Since the selected model for inflammasome activation is closely related to the particulate size, it is reasonable to link the consequences of THP-1 cells in response to Chry and LIB with their remarkably different physical sizes. Chrysotile fibers belong to the group of longer and thinner fibers; the length of Chry is about 3 times that of LIB, and the mean surface area is about 5–6 times that of LIB (see Table 1), suggesting that Chry has more potential to result in aggressive lysosomal rupture and subsequent activation of the NLRP3 inflammasome. It has been well-demonstrated that longer fibers are incapable of undergoing phagocytosis in vitro and in animals [21]. Long fibers have a greater potency than short fibers in assays of pro-inflammatory and genotoxic activity [53], and stimulate greater release of IL-1β by macrophages [5]. Therefore, further study of the correlations between particle size and activation of the inflammasome would be particularly interesting. In contrast, LIB probably stimulates more ROS production via a tightly controlled ROS-mediated model [51] in which, ROS primes NLRP3 on the one hand, but may impact inflammasome activation and down-regulate caspase-1 activity on the other hand.

4.3. Signaling cascade in BEAS-2B cells mediated by the conditioned medium

We have demonstrated that IL-1β is a major player in THP-1 conditioned medium, leading to the initiation of the inflammatory response in the BEAS-2B cells. Besides IL-1β, we also detected lipids peroxides in conditioned medium (Fig. 4D) which is possibly another "alarm" signal that triggers responses in BEAS-2B. However, this should be specifically identified and confirmed in future studies.

Combining our findings with those from others, the process through which IL-1β triggers BEAS-2B release of IL-6 likely consists

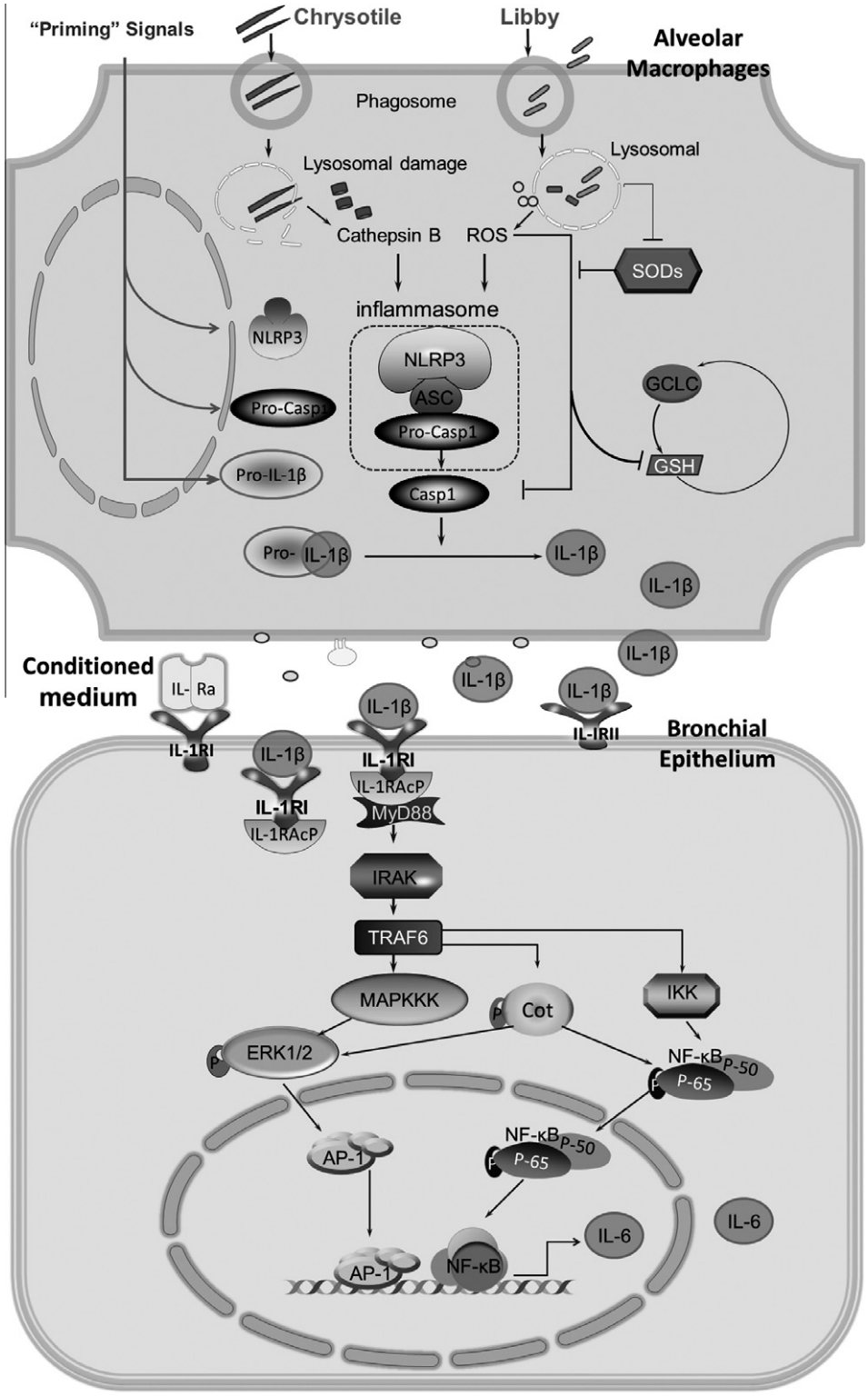

Fig. 9. Proposed schema for Chry and LIB induced signal transduction from the macrophage to the epithelium. In the macrophage "priming" step, the pro-inflammatory signals mediate activation of receptors and induction of NLRP3, procaspase-1 and pro-IL-1β. When macrophages are exposed to chrysotile fibers, phagocytosis is followed by phagosomal destabilization and lysosomal rupture. Lysosomal damage results in the release of cathepsin B into the cytosol that triggers three members of NLRP3 inflammasome to assemble and subsequent activation of ASC (apoptosis-associated speck-like protein containing a CARD). This second step eventually activates pro-caspase-1, which in turn cleaves pro-IL-1β. In comparison to chrysotile, the relatively smaller size of the Libby amphibole probably results in more ROS production via a tightly controlled ROS-mediated model in which, ROS activate NLRP3, although high oxygen tension can also impact inflammasome function and down-regulate caspase-1 activity. In the epithelial cell, IL-1β signal transduction is initiated through a ligand-induced conformational change in the first extracellular domain of the IL-1RI that facilitates recruitment of IL-1RacP. Meanwhile, IL-1Ra can block the IL-1β signaling. The trimetric complex rapidly assembles two intracellular signaling proteins, MYD88, and IRAK, then through TRAF6 (TNF receptor-associated factor 6) linked to the downstream protein kinase cascades, including MAPK kinase family, Cot and IκB kinases (IKKs). The activation of ERK1/2 or other MAPKs leads to activation of the AP-1 transcription factor; the IKKβ-mediated phosphorylation of p65 modulates NF-κB activity. Both AP-1 and NF-κB can directly up-regulate its target gene, IL-6. IL-6 further contributes to asbestos-related pathological phenotypes, such as asbestosis, lung cancer, and mesothelioma.

of the following steps, as illustrated in Fig. 9. The initial step in IL-1β signal transduction is a ligand-induced conformational change in the first extracellular domain of the IL-1RI that facilitates recruitment of IL-1RacP. Through conserved cytosolic regions called Toll- and IL-1R-like (TIR) domains, the trimetric complex rapidly assembles two intracellular signaling proteins, myeloid differentiation primary response gene 88 (MYD88) and interleukin-1 receptor–activated protein kinase (IRAK) [41]. The IL-1R–TLR receptor-mediated signals, which are linked to the downstream protein kinase cascades, have been studied extensively. Members of the MAPK kinase (MAPKKK; called MAP3 K here) family, including MEKK1, 2, 3 and Cot (Tpl2 or MAP3K8) are critical in this process [54–56]. The activation of ERK1/2 or other MAPKs leads to activation of the AP-1 transcription factor, which could directly up-regulate its target gene, IL-6. In addition, the IKKβ-mediated phosphorylation of p65 at Ser536 requires the upstream kinases Cot (Tpl2) and PKCζ [57]. Then, in turn, IL-6 may act as a significant autocrine growth factor in epithelial cells [58,59] to further induce asbestos-related pathological phenotypes, such as asbestosis, lung cancer, and mesothelioma.

5. Conclusion

We have investigated the signal transduction from the THP-1 macrophages to bronchial epithelial cells (BEAS-2B) in response to Chry and LIB through direct treatments of THP-1 cells followed by THP-1 conditioned medium treatments of BEAS-2B. We found that direct treatments of THP-1 cells with Chry and LIB differentially activated the inflammasome in processing IL-1β. IL-1β in conditioned medium acts as a secondary mediator to trigger BEAS-2B cells signaling cascades, including ERK, Cot, and then AP-1 and NF-kB, to induce IL-6, which then leads epithelial cells to pathologic phenotypes. Using IL-1Ra could interrupt the interaction and may have a potential therapeutic effect when exposure to pathogenic particles occurs.

Acknowledgements

The authors thank Brooke T. Mossman, Arti Shukla, Maximilian B. MacPherson, and Jedd Hillegass for helpful discussions.

Appendix A. Supplementary material

Supplementary data associated with this article can be found, in the online version, at http://dx.doi.org/10.1016/j.cyto.2012.08.025.

References

[1] Agency for Toxic Substances and Disease Registry. Asbestos: Health Effects, Retrieved April 10; 2009. <http://www.atsdr.cdc.gov/asbestos/asbestos/health_effects/index.html>.
[2] Martinez FO, Helming L, Gordon S. Alternative activation of macrophages: an immunologic functional perspective. Annu Rev Immunol 2009;27:451–83.
[3] Dostert C, Petrilli V, Van Bruggen R, Steele C, Mossman BT, Tschopp J. Innate immune activation through Nalp3 inflammasome sensing of asbestos and silica. Science 2008;320:674–7.
[4] Cassel SL, Eisenbarth SC, Iyer SS, Sadler JJ, Colegio OR, Tephly LA, et al. The Nalp3 inflammasome is essential for the development of silicosis. Proc Nat Acad Sci 2008;105:9035–40.
[5] Palomäki J, Välimäki E, Sund J, Vippola M, Clausen PA, Jensen KA, et al. Long, needle-like carbon nanotubes and asbestos activate the NLRP3 inflammasome through a similar mechanism. ACS Nano 2011;5:6861–70.
[6] Kummer JA, Broekhuizen R, Everett H, Agostini L, Kuijk L, Martinon F, et al. Inflammasome components NALP 1 and 3 show distinct but separate expression profiles in human tissues suggesting a site-specific role in the inflammatory response. J Histochem Cytochem 2007;55:443–52.
[7] Martinon F, Mayor A, Tschopp J. The inflammasomes: guardians of the body. Annu Rev Immunol 2009;27:229–65.
[8] Hornung V, Bauernfeind F, Halle A, Samstad EO, Kono H, Rock KL, et al. Silica crystals and aluminum salts activate the NALP3 inflammasome through phagosomal destabilization. Nat Immunol 2008;9:847–56.
[9] Flavell RA, Elinav E, Hu B, Sutterwala F, Eisenbarth S. KL1 the inflammasome in health and disease. Cytokine 2010;52:2.
[10] Peters M, Meyer zum Büschenfelde K-H, Rose-John S. The function of the soluble IL-6 receptor in vivo. Immunol Lett 1996;54:177–84.
[11] Haegens A, van der Vliet A, Butnor KJ, Heintz N, Taatjes D, Hemenway D, et al. Asbestos-induced lung inflammation and epithelial cell proliferation are altered in myeloperoxidase-null mice. Cancer Res 2005;65:9670–7.
[12] Shukla A, Lounsbury KM, Barrett TF, Gell J, Rincon M, Butnor KJ, et al. Asbestos-induced peribronchiolar cell proliferation and cytokine production are attenuated in lungs of protein kinase C-delta knockout mice. Am J Pathol 2007;170:140–51.
[13] Simeonova PP, Toriumi W, Kommineni C, Erkan M, Munson AE, Rom WN, et al. Molecular regulation of IL-6 activation by asbestos in lung epithelial cells: role of reactive oxygen species. J Immunol 1997;159:3921–8.
[14] Cummins AB, Palmer C, Mossman BT, Taatjes DJ. Persistent localization of activated extracellular signal-regulated kinases (ERK1/2) is epithelial cell-specific in an inhalation model of asbestosis. Am J Pathol 2003;162:713–20.
[15] Wang X, Samet J, Ghio A. Asbestos-induced activation of cell signaling pathways in human bronchial epithelial cells. Exp Lung Res 2006;32:229–43.
[16] Robledo RF, Buder-Hoffmann SA, Cummins AB, Walsh ES, Taatjes DJ, Mossman BT. Increased phosphorylated extracellular signal-regulated kinase immunoreactivity associated with proliferative and morphologic lung alterations after chrysotile asbestos inhalation in mice. Am J Pathol 2000;156:1307–16.
[17] Drumm K, Messner C, Kienast K. Reactive oxygen intermediate-release of fibre-exposed monocytes increases inflammatory cytokine-mRNA level, protein tyrosine kinase and NF-κB activity in co-cultured bronchial epithelial cells (BEAS-2B). Eur J Med Res 1999;4:257–63.
[18] Kienast K, Kaes C, Drumm K, Buhl R, Micke P, Oesch F, et al. Asbestos-exposed blood monocytes–deoxyribonucleic acid strand lesions in co-cultured bronchial epithelial cells. Scand J Work Environ Health 2000;26:71–7.
[19] Herseth JI, Refsnes M, Lag M, Hetland G, Schwarze PE. IL-1β as a determinant in silica-induced cytokine responses in monocyte-endothelial cell co-cultures. Hum Exp Toxicol 2008;27:387–99.
[20] Gunter ME, Belluso E, Mottana A. Amphiboles: environmental and health concerns. Rev Mineral Geochem 2007;67:453–516.
[21] Campbell WJ, Huggins CW, Wylie AG. Chemical and physical characterization of amosite, chrysotile, crocidolite, and nonfibrous tremolite for oral ingestion studies by the National Institute of Environmental Health. Sciences 1980;8452:1–63.
[22] Bandli BR, Gunter ME. A review of scientific literature examining the mining history, geology, mineralogy, and amphibole asbestos health effects of the Rainy Creek igneous complex, Libby, Montana, USA. Inhal Toxicol 2006;18:949–62.
[23] Meeker GP, Bern AM, Brownfield IK, Lowers HA, Sutley SJ, Hoefen TM, et al. The composition and morphology of amphibole from the Rainy Creek Complex, near Libby, Montana. Am. Mineral. 2003;88:1955–69.
[24] Bellamy JM, Gunter ME. Morphological characterization of Libby "six-mix" used in in vivo studies. Periodico Di Mineralogia 2008;77:75–82.
[25] Schwende H, Fitzke E, Ambs P, Dieter P. Differences in the state of differentiation of THP-1 cells induced by phorbol ester and 1,25-dihydroxyvitamin D3. J Leukoc Biol 1996;59:555–61.
[26] Tsuchiya S, Kobayashi Y, Goto Y, Okumura H, Nakae S, Konno T, et al. Induction of maturation in cultured human monocytic leukemia cells by a phorbol diester. Cancer Res 1982;42:1530–6.
[27] Churg A, Wiggs B. Fiber size and number in workers exposed to processed chrysotile asbestos, chrysotile miners, and the general population. Am J Ind Med 1986;9:143–52.
[28] Groppo C, Tomatis M, Turci F, Gazzano E, Ghigo D, Compagnoni R, et al. Potential toxcity of nonregulated asbestiform minerals: balangeroite from the Western Alps. Part 1: identification and characterization. J Toxicol Environ Health A 2005;68:1–19.
[29] Hillegass J, Shukla A, MacPherson M, Lathrop S, Alexeeva V, Perkins T, et al. Mechanisms of oxidative stress and alterations in gene expression by Libby six-mix in human mesothelial cells. Parti Fibre Toxicol 2010;7:26.
[30] Valentine R, Chang MJ, Hart RW, Finch GL, Fisher GL. Thermal modification of chrysotile asbestos: evidence for decreased cytotoxicity. Environ Health Perspect 1983;51:357–68.
[31] Shukla A, MacPherson MB, Hillegass J, Ramos-Nino ME, Alexeeva V, Vacek PM, et al. Alterations in gene expression in human mesothelial cells correlate with mineral pathogenicity. Am J Respir Cell Mol Biol 2009;41:114–23.
[32] Li M, Chiu JF, Mossman BT, Fukagawa NK. Down-regulation of manganese-superoxide dismutase through phosphorylation of FOXO3a by Akt in explanted vascular smooth muscle cells from old rats. J Biol Chem 2006;281:40429–39.
[33] Li M, Chiu JF, Kelsen A, Lu SC, Fukagawa NK. Identification and characterization of an Nrf2-mediated ARE upstream of the rat glutamate cysteine ligase catalytic subunit gene (GCLC). J Cell Biochem 2009;107:944–54.
[34] Blake DJ, Bolin CM, Cox DP, Cardozo-Pelaez F, Pfau JC. Internalization of Libby amphibole asbestos and induction of oxidative stress in murine macrophages. Toxicol Sci 2007;99:277–88.
[35] Haegens A, Barrett TF, Gell J, Shukla A, MacPherson M, Vacek P, et al. Airway epithelial NF-κB activation modulates asbestos-induced inflammation and mucin production in vivo. J Immunol 2007;178:1800–8.

[36] Ramos-Nino ME, Haegens A, Shukla A, Mossman BT. Role of mitogen-activated protein kinases (MAPK) in cell injury and proliferation by environmental particulates. Mol Cell Biochem 2002;234–235:111–8.
[37] Johannessen CM, Boehm JS, Kim SY, Thomas SR, Wardwell L, Johnson LA, et al. COT drives resistance to RAF inhibition through MAP kinase pathway reactivation. Nature 2010;468:968–72.
[38] Buss H, Dörrie A, Schmitz ML, Hoffmann E, Resch K, Kracht M. Constitutive and interleukin-1-inducible phosphorylation of p65 NF-κB at Serine 536 is mediated by multiple protein kinases including IκB kinase (IKK)-α, IKKβ, IKKϵ, TRAF Family member-associated (TANK)-binding kinase 1 (TBK1), and an unknown kinase and couples p65 to TATA-binding protein-associated factor II31-mediated interleukin-8 transcription. J Biol Chem 2004;279: 55633–43.
[39] Arend WP, Palmer G, Gabay C. IL-1, IL-18, and IL-33 families of cytokines. Immunol Rev 2008;223:20–38.
[40] Bergsbaken T, Fink SL, Cookson BT. Pyroptosis: host cell death and inflammation. Nat Rev Micro 2009;7:99–109.
[41] Weber A, Wasiliew P, Kracht M. Interleukin-1 (IL-1) pathway. Sci Signal 2010;3:cm1.
[42] Bauernfeind F, Ablasser A, Bartok E, Kim S, Schmid-Burgk J, Cavlar T, et al. Inflammasomes: current understanding and open questions. Cell Mol Life Sci 2010:1–19.
[43] Bauernfeind FG, Horvath G, Stutz A, Alnemri ES, MacDonald K, Speert D, et al. Cutting edge: NF-κB activating pattern recognition and cytokine receptors license NLRP3 inflammasome activation by regulating NLRP3 expression. J Immunol 2009;183:787–91.
[44] Gong Y-N, Wang X, Wang J, Yang Z, Li S, Yang J, et al. Chemical probing reveals insights into the signaling mechanism of inflammasome activation. Cell Res 2010;20:1289–305.
[45] Bauernfeind F, Bartok E, Rieger A, Franchi L, Núñez G, Hornung V. Cutting edge: reactive oxygen species inhibitors block priming, but not activation, of the NLRP3 inflammasome. J Immunol 2011;187:613–7.
[46] Bryant C, Fitzgerald KA. Molecular mechanisms involved in inflammasome activation. Trends Cell Biol 2009;19:455–64.
[47] Tschopp J, Schroder K. NLRP3 inflammasome activation: the convergence of multiple signalling pathways on ROS production? Nat Rev Immunol 2010;10:210–5.
[48] Romani L, Fallarino F, De Luca A, Montagnoli C, D'Angelo C, Zelante T, et al. Defective tryptophan catabolism underlies inflammation in mouse chronic granulomatous disease. Nature 2008;451:211–5.
[49] van de Veerdonk FL, Smeekens SP, Joosten LAB, Kullberg BJ, Dinarello CA, van der Meer JWM, et al. Reactive oxygen species–independent activation of the IL-1β inflammasome in cells from patients with chronic granulomatous disease. Proc Nat Acad Sci 2010;107:3030–3.
[50] Meissner F, Molawi K, Zychlinsky A. Superoxide dismutase 1 regulates caspase-1 and endotoxic shock. Nat Immunol 2008;9:866–72.
[51] Latz E. The inflammasomes: mechanisms of activation and function. Curr Opin Immunol 2010;22:28–33.
[52] Schroder K, Tschopp J. The Inflammasomes. Cell 2010;140:821–32.
[53] Donaldson K, Murphy F, Duffin R, Poland C. Asbestos, carbon nanotubes and the pleural mesothelium: a review of the hypothesis regarding the role of long fibre retention in the parietal pleura, inflammation and mesothelioma. Part Fibre Toxicol 2010;7:5.
[54] Huang Q, Yang J, Lin Y, Walker C, Cheng J, Liu ZG, et al. Differential regulation of interleukin 1 receptor and Toll-like receptor signaling by MEKK3. Nat Immunol 2004;5:98–103.
[55] Dumitru CD, Ceci JD, Tsatsanis C, Kontoyiannis D, Stamatakis K, Lin J-H, et al. TNF-α induction by LPS is regulated posttranscriptionally via a Tpl2/ERK-dependent pathway. Cell 2000;103:1071–83.
[56] Handoyo H, Stafford MJ, McManus E, Baltzis D, Peggie M, Cohen P. IRAK1-independent pathways required for the interleukin-1-stimulated activation of the Tpl2 catalytic subunit and its dissociation from ABIN2. Biochem J 2009;424:109–18.
[57] Viatour P, Merville M-P, Bours V, Chariot A. Phosphorylation of NF-κB and IκB proteins: implications in cancer and inflammation. Trends Biochem Sci 2005;30:43–52.
[58] Miki S, Iwano M, Miki Y, Yamamoto M, Tang B, Yokokawa K, et al. Interleukin-6 (IL-6) functions as an in vitro autocrine growth factor in renal cell carcinomas. FEBS Lett 1989;250:607–10.
[59] Yeh HH, Lai WW, Chen HHW, Liu HS, Su WC. Autocrine IL-6-induced Stat3 activation contributes to the pathogenesis of lung adenocarcinoma and malignant pleural effusion. Oncogene 2006;25:4300–9.